Talanta 117 (2013) 127–132

Contents lists available at ScienceDirect

Talanta

journal homepage: www.elsevier.com/locate/talanta

Detection of Hg^{2+} based on the selective inhibition of peroxidase mimetic activity of BSA-Au clusters

Rui Zhu [a], Yan Zhou [b], Xi-Liang Wang [a], Li-Ping Liang [a], Yi-Juan Long [a], Qin-Long Wang [a], Hai-Jie Zhang [a], Xiao-Xiao Huang [a], Hu-Zhi Zheng [a,*]

[a] The Key Laboratory of Luminescence and Real-time Analysis (Southwest University), Ministry of Education, College of Chemistry and Chemical Engineering, Southwest University, Chongqing 400715, PR China
[b] Southwest University Library, Southwest University, Chongqing 400715, PR China

ARTICLE INFO

Article history:
Received 16 May 2013
Received in revised form
22 August 2013
Accepted 28 August 2013
Available online 3 September 2013

Keywords:
BSA-Au clusters
Hg^{2+}
Peroxidase-like activity
Detection

ABSTRACT

It was found that Hg^{2+} can inhibit the peroxidase mimetic activity of bovine serum albumin (BSA) protected Au clusters (BSA-Au) due to the specific interaction between Hg^{2+} and Au^{+} existed onto the surface of BSA-Au clusters. By coupling with 3, 3′, 5, 5′-tetramethylbenzidine (TMB)–H_2O_2 chromogenic reaction, a novel method for Hg^{2+} detection was developed based on the inhibiting effect of Hg^{2+} on BSA-Au clusters peroxidase-like activity. This method exhibited high selectivity and sensitivity. As low as 3 nM (0.6 ppb, 3σ) Hg^{2+} could be detected with a linear range from 10 nM (2 ppb) to 10 μM (2 ppm) and this method was successfully applied for the determination of total mercury content in skin lightening products.

1. Introduction

Recently, the study and application of peroxidase-like nanomaterials has been of great interest. Many nanomaterials, such as iron oxide [1], graphene oxide (GO) [2], carbon nanotubes [3], carbon dots [4], bimetallic alloy nano-structures [5], gold nanoparticles [6], sheet-like and spherical FeS nanostructures [7], have been demonstrated to be mimetic peroxidases. These enzyme-like nanomaterials are more stable against denaturation or protease digestion than natural enzymes. Furthermore, their preparation or storage is relatively simple and low-cost. Wei et al. [8] applied peroxidase-like Fe_3O_4 magnetic nanoparticles to H_2O_2 and glucose detection. Song et al. [2] detected glucose based changing of GO peroxidase mimetic activity. Long et al. [9] found that Hg^{2+} can improve the catalytic activity of gold nanoparticles (AuNPs) and hence enable the detection of Hg^{2+}. However, to the best of our knowledge, there are few reports involved in the inhibition of peroxidase mimetic activity of nanomaterials. Recently, Tseng et al. reported the determination of Hg^{2+} based on the inhibition of the peroxidase-like activity of Pt-Au nanoparticles [10].

Xie prepared BSA-Au clusters in 2009 via a simple and green method [11]. Such BSA-Au clusters possessed a strong fluorescence (maximal emission at 640 nm, fluorescence quantum yield ca. 6%). Furthermore, it was found that the fluorescence of BSA-Au clusters can be quenched by Cu^{2+} [12]and Hg^{2+} [13], and hence, detection of Cu^{2+} or Hg^{2+} was accomplished. Subsequently, Wang et al. found BSA-Au clusters exhibited highly peroxidase-like activities [14]. Compared with other reported nanoparticles, which have peroxidase mimetic activities, BSA-Au clusters are small in size, highly biocompatible, and stable.

Mercury compounds can inactivate tyrosinase and delay the formation of melanin, resulting in a lighter skin tone. Hence, they can be used in cosmetics for the ability of skin whitening [15,16]. But after long-term use of these lightening cosmetics, mercury compounds would deposit in the bone, resulting in damage of the digestive and excretory system, and leading to deafness, arthritis, and ankylosing spondylitis disease [17]. Excessive mercury compounds in cosmetics endanger women who use these cosmetics over an extended period of time. Many countries limit the maximum level of total mercury in cosmetics, for example, the maximum level of total mercury in cosmetics permitted by Ministry of Health of the People's Republic of China is 1 ppm [18]. Currently, atomic absorption spectrometry (AAS) [19] and atomic fluorescence spectrometry (AFS) [20] are widely used for the detection of mercury in cosmetics. However these methods cannot realize naked-eyed screening and in situ detection. Therefore, it is highly desirable to develop a inexpensive method that can realize naked-eyed screening and in situ detection of total mercury in cosmetics.

Herein, we found that Hg^{2+} could selectively inhibit the peroxidase mimetic activity of BSA-Au clusters, reducing their ability to

* Corresponding author. Tel.: +86 23 6825 2360; fax: +86 23 6825 4000.
E-mail address: zhenghz@swu.edu.cn (H.-Z. Zheng).

0039-9140/$ - see front matter © 2013 Elsevier B.V. All rights reserved.
http://dx.doi.org/10.1016/j.talanta.2013.08.053

catalyze the chromogenic reaction of TMB and hydrogen peroxide. Based on this phenomenon, semi-quantitative determination of Hg^{2+} via visual observation and quantitative determination of Hg^{2+} via absorption were achieved. This proposed method shows high selectivity for the specific interaction between Hg^{2+} and Au^{+} onto surfaces of BSA-Au clusters. At the same time, this method is highly sensitive because little change in enzyme activity has a significant impact on chromogenic reaction. The mercury content in cosmetics can be detected by our method after digestion.

2. Experimental

2.1. Chemical and materials

$HAuCl_4$ was purchased from Aladdin Reagent Co., Ltd. (Shanghai, China). NaOH was purchased from Chongqing Pharmaceutical Co., Ltd. (Chongqing, China). BSA, TMB, ethylene diamine tetraacetic acid (EDTA) and $NaBH_4$ were purchased from Beijing Dingguo Changsheng Biotechnology Co., Ltd (Beijing, China). $Hg(NO_3)_2$ was purchased from the Guizhou Lee Cheung Mercury Industry Co. Ltd (Guiyang, China). H_2O_2 (30%), HNO_3, H_2SO_4 and HCl were all purchased from Chongqing Chuandong Chemical Co., Ltd. (Chongqing, China). Two kinds of skin lightening creams were obtained in the local market. Ultrapure water (18.2 M) was prepared with a Milli-Q system (USA) and used in all experiments.

2.2. Synthesis of BSA-Au clusters

BSA-Au clusters were prepared according to a reported method [11]. All glassware was washed with Aqua Regia (HCl: HNO_3 volume ratio=3:1), and rinsed with ultrapure water. In a typical experiment, aqueous $HAuCl_4$ solution (5 mL, 10 mM) was mixed with BSA solution (5 mL, 50 mg/mL) under vigorous stirring at 37 °C. NaOH solution (0.5 mL, 1 M) was introduced 2 min later, and the reaction was allowed to proceed under vigorous stirring at 37 °C for 12 h. The final solution was stored at 4 °C in refrigerator until use.

2.3. Digestion of cosmetics

Two different skin lightening creams were digested according to a standard procedure (GB/T 7917.1-1987, PR China) [18]. One skin lightening cream is an unqualified product which contains mercury levels far higher than acceptable limits in China. The other is a commercially qualified product. Briefly, 5 mL of concentrated HNO_3 and 1 mL of H_2O_2 were mixed with 1 g of the cosmetic products. After reaction at room temperature for 30 min, the solutions were heated in a boiling water bath for another 2 h. At last, the cooled solution was diluted to 50 mL with 10% H_2SO_4. The total mercury in cosmetic product was transferred into Hg^{2+} after digestion.

2.4. Detection of Hg^{2+}

A typical procedure for Hg^{2+} detection was described below. At room temperature, 100 μL of 0.2 M NaAc buffer solutions (pH 4.0) and 50 μL of 4 mM (expressed in concentration of Au atoms) as-prepared BSA-Au clusters were pipetted into a 1.5 mL vial, and then Hg^{2+} solutions with different concentrations were added. After 10 min of incubation, 100 μL of 1.5 mM TMB and 100 μL of 50 mM H_2O_2 were added. The mixtures were finally diluted to 1 mL and incubated for another 15 min at 40 °C. The absorbance at 652 nm was recorded by a UV-2450-PC spectrophotometer (Shimadzu, Japan) for the quantitative determination of Hg^{2+}. A digital camera (A630, Canon) was used to obtain images of samples for semi-quantitative determination.

2.5. AFS determination

To estimate the accuracy of this method, we measured the Hg^{2+} concentration in the digested sample and compared our results with the AFS method. We added 0, 0.2, 0.4, 0.6, 0.8, and 1.0 mL of 0.5 μM Hg^{2+} standard solutions into 5 mL HCl, and diluted them to 50 mL. We created a standard curve by recording the six data and calculated the mercury levels in each cosmetic product. AFS signals were recorded by an AFS-230E Atomic Fluorescence Spectrophotometer (Beijing Haiguang Instrument Co. Ltd., Beijing, China).

2.6. X-ray photoelectron spectroscopy (XPS) measurement

XPS spectra were collected using an ESCALAB250 X-ray photoelectron spectroscope (Thermo, UK). BSA-Au clusters solution, both with and without Hg^{2+}, were dropped on a Si substrate and oven-dried before measurement.

2.7. Electron paramagnetic resonance (EPR) measurement

EPR signals were measured by a Bruker ESP 300E spectrometer (Bruker, Rheinstetten, Germany) with a microwave bridge (receiver gain, 1×10^5; modulation amplitude, 2 Gauss; microwave power, 10 mW; modulation frequency, 100 kHz). A sample containing 0.2 M dimethyl pyridine N-oxide (DMPO) was transferred to a quartz capillary tube and placed in the EPR cavity. Under the UV-irradiation at 355 nm, an EPR signal was detected using DMPO as the spin trap.

2.8. The inhibition effect of $NaBH_4$ on the peroxidase-like activity of BSA-Au cluster

To determine whether Au^{+} is the key to peroxidase mimetic activity of BSA-Au clusters, different concentrations of $NaBH_4$ (0, 0.5, 1, 5, 10, 50, and 100 μM) were mixed with BSA-Au clusters. The buffer (pH 4.0) was then added into the solution and incubated at 40 °C for 30 min. TMB and H_2O_2 were added as described in 2.4. The absorbance changes in 652 nm were recorded.

3. Results and discussions

3.1. Selective inhibition effect of Hg^{2+} on the peroxidase mimetic activity of BSA-Au clusters

BSA-Au clusters possessing a high peroxidase mimetic activity, can catalyze the chromogenic reaction of TMB and H_2O_2, which produces a product with a significant absorbance at 652 nm (Fig. 1, Curve 1). However, after the addition of 50 μM (10 ppm) Hg^{2+}, as high as 200 μM of BSA-Au clusters can hardly catalyze the chromogenic reaction of TMB and H_2O_2 (Fig. 1, Curve 2). It means that Hg^{2+} can inhibit the catalytic activity of BSA-Au clusters. EDTA can chelate with Hg^{2+}, and hence reduce the inhibition of catalytic activity of BSA-Au clusters (Fig. 1, Curve 3).

The peroxidase-like activity of BSA-Au clusters and the inhibiting effect of Hg^{2+} on the peroxidase-like activity can be further certified by EPR measurement. As Fig. S1 shows, the signal intensity of $\cdot OH$ radicals generated by ultra-violet irradiation of H_2O_2 increased with the addition of BSA-Au clusters, which is a typical behavior of peroxidase [14]. In the presence of Hg^{2+}, the EPR signal intensity decreases. This result also demonstrates that Hg^{2+} can inhibit the peroxidase-like activity of BSA-Au clusters.

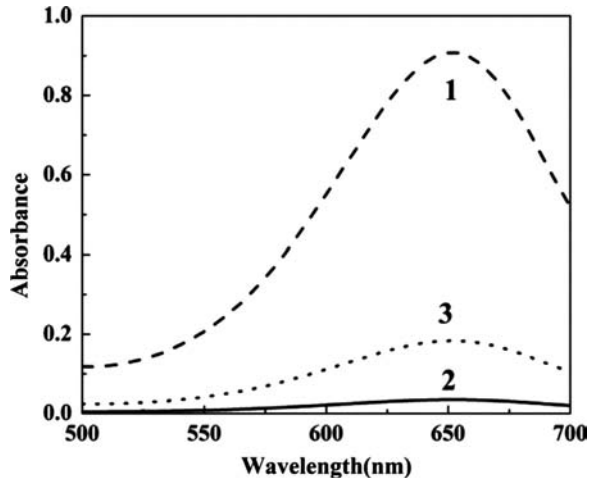

Fig. 1. Inhibiting effects of Hg^{2+} on the peroxidase mimetic activity of BSA-Au clusters. 1, 150 μM TMB+5 mM H_2O_2+200 μM BSA-Au clusters; 2, 1+50 μM Hg^{2+}; 3, 1+50 μM Hg^{2+}+50 μM EDTA; pH=4.0.

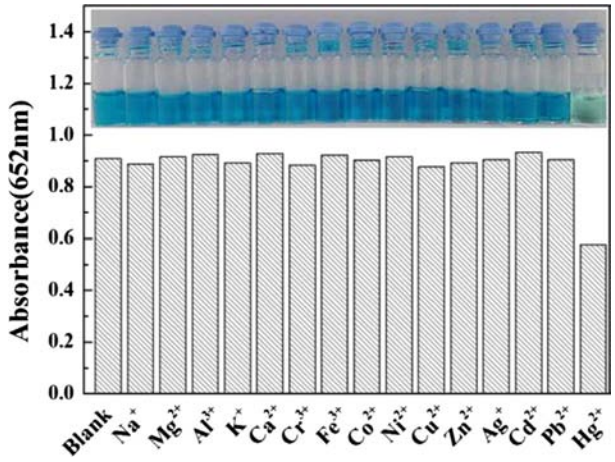

Fig. 2. Effects of metal ions on the peroxidase-like activity of BSA-Au clusters. Concentration of Na^+, Fe^{3+}, Co^{2+}, and Ag^+ are 50 μM; concentration of Al^{3+}, K^+, Ca^{2+}, Cr^{3+}, Ni^{2+}, Cu^{2+}, Zn^{2+}, Cd^{2+}, Pb^{2+}, and Mg^{2+} are 100 μM; concentration of Hg^{2+} is 1.0 μM. BSA-Au clusters, 200 μM; TMB, 150 μM; H_2O_2, 5 mM; pH 4.0; temperature 40 °C.

By adopting TMB-H_2O_2 chromogenic reaction to evaluate the peroxidase-like activity of BSA-Au clusters, effects of common metal ions on the catalytic activity were investigated. As shown in Fig. 2, 50 μM of Na^+, Fe^{3+}, Co^{2+}, Ag^+, and 100 μM of Mg^{2+}, Al^{3+}, K^+, Ca^{2+}, Cr^{3+}, Ni^{2+}, Cu^{2+}, Zn^{2+}, Cd^{2+}, and Pb^{2+} have no effect on the peroxidase-like activity of BSA-Au cluster. However, 1.0 μM (0.2 ppm) of Hg^{2+} causes ca. 30% decrease in absorbance. This phenomenon is caused by two reasons, one of which is that Hg^{2+} inhibits the catalytic activity, the other is the presence of Hg^{2+} leads to the fusion of clusters to aggregate which certified by dynamic light scattering results (Fig. S2). Interestingly, this inhibition can be detected visually. These results confirm that the inhibiting effect of Hg^{2+} on the peroxidase-like activity of BSA-Au clusters is highly selective.

As reported by Xie, the small amount of Au^+ (ca. 17%) present on the surface of the Au core helped to stabilize the BSA-Au cluster [11]. $NaBH_4$ is a strong reductant which can reduce Au^+ to Au^0. After the addition of $NaBH_4$, the peroxidase-like activity of BSA-Au decreased (Fig. S3). The activity decreases with the concentration of $NaBH_4$ increasing. Hence, we suppose that the peroxidase mimetic active sites of BSA-Au clusters are Au^+ on their surfaces. Any compounds that bind with Au^+ will cause a change in catalytic activity. As confirmed by others groups [21,22], Hg^{2+} can interact with Au^+ with high specificity. In the previous report [12], it was shown that Cu^{2+} can also interact with BSA-Au cluster. Cu^{2+}, however, did not affect the catalytic activity (Figs. 2, S4), because Cu^{2+} -induced fluorescence quenching is due to its binding with BSA rather than metal–metal interaction as in the case of Hg^{2+}. As a result, Hg^{2+} inhibits the peroxidase-like activity of BSA-Au clusters with higher selectivity than the fluorescence quenching method [13] (Fig. 3). Furthermore, XPS was used to demonstrate the supposition. It was revealed that there were Au^0 and Au^+ in BSA-Au clusters (Fig. S5a). The peak position, full width at half maximum (FWHM) and peak area of Au^0 and Au^+ clearly changed in the presence of Hg^{2+} (Fig. S5b). The binding of Hg^{2+} to BSA-Au clusters was also confirmed (Fig. S5c). All these results demonstrated that Hg^{2+} can bind with Au^+ on the surfaces of BSA-Au clusters and change the binding energy of Au^+ [23–25]. The change in binding energy causes a change in the catalytic activity of BSA-Au clusters [26].

Long et al. [9] found that it is Hg^0 as opposed to Hg^{2+} that causes the change of surface properties of AuNPs and improves its catalytic activity. They suppose that two steps are involved in the specific enhancement of Hg^0. First, Hg^{2+} is reduced to Hg^0 by sodium citrate, which acts as both the reducing and the capping agents during the preparation of AuNPs; second, Hg^0 disperses on the surface of AuNPs and thus changes the surface properties of AuNPs. As a result, the peroxidase-like activity of AuNPs improves. In our method, we suppose that the peroxidase mimetic active sites of BSA-Au clusters are Au^+ on their surfaces, and Hg^{2+} inhibits the peroxidase-like activity of BSA-Au clusters with high selectivity for the specific interaction between Au^+ and Hg^{2+}.

3.2. Optimization of determining conditions

The selective inhibition of Hg^{2+} on the peroxidase-like activity of BSA-Au clusters led to a significant decrease in the absorbance at 652 nm of TMB-H_2O_2 chromogenic system. Furthermore, with increasing Hg^{2+}, the absorbance of TMB-H_2O_2 chromogenic system decreases. The Hg^{2+} concentration-dependent inhibition of BSA-Au cluster catalytic activity provides a potential strategy for Hg^{2+} detection. We used A_0/A as a criterion to optimize the detection conditions, where A_0 and A is the absorbance in the absence and presence of Hg^{2+}, respectively.

The catalytic activity of BSA-Au clusters is pH and temperature-dependent. Here, we measured the peroxidase-like activity of BSA-Au clusters while varying the pH from 1 to 12, and the temperature from 20 °C to 60 °C. The effects of these two parameters on the catalytic relative activity of TMB oxidation are shown in Figs. S6 and S7, respectively. The results showed that

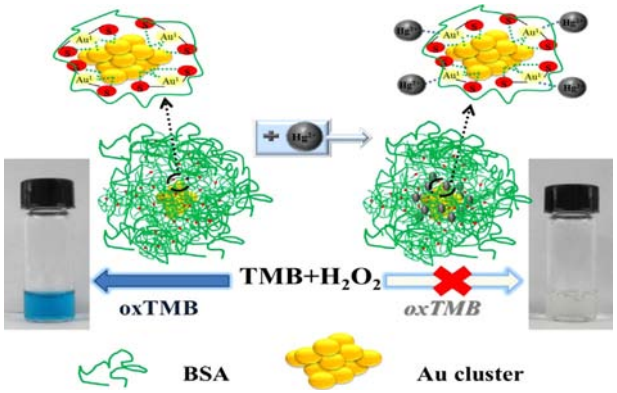

Fig. 3. Schematic diagram of Hg^{2+} detection.

the optimal pH is 4.0 and the temperature is 40 °C. Our optimal pH value is similar to other reports that using TMB as substrate. The optimal pH of TMB-H_2O_2 system catalyzed by other kinds of nanomaterials is also at the same range [2]. This optimal pH value seems to be related to characteristics of H_2O_2 and the TMB-H_2O_2 chromogenic reaction. Under higher pH condition, H_2O_2 becomes unstable and tends to decompose into H_2O and O_2, and is hard to produce reactive radical species [27]. However, the TMB-H_2O_2 chromogenic reaction would be inhibited at a lower pH (pH < 3) level. Sulfuric acid was usually used as a stop reagent for the TMB-H_2O_2 chromogenic reaction. Therefore, a pH level of 4.0 is optimal. If the temperature is higher than 40 °C, the structure of BSA would alter. The content in the short-segment chains connecting α-helical segments of BSA decreases with loss of tertiary structure around 57 °C [28]. We also found that the white turbidity appeared within 15 min in heated (55 °C) BSA-Au clusters solution, and it increased with increase in heating time. The TMB-H_2O_2 chromogenic reaction proceeds slowly at low temperatures (less than 40 °C). Thus, we adopted 40 °C as the optimal condition for subsequent analysis experiments to get better sensitivity.

A strong dependence was found between the value A_0/A and concentrations of BSA-Au clusters, TMB or H_2O_2. They had a common tendency that the value A_0/A gradually increased with concentrations at lower levels until they reached the maximum. The optimal concentration of BSA-Au clusters, TMB, and H_2O_2 are 200 μM, 150 μM, and 5 mM, respectively (Figs. S8–S10). The results indicated that the sensitivity of the proposed method would be limited to high concentrations of BSA-Au clusters, TMB or H_2O_2.

The optimal time for the incubation of Hg^{2+} with BSA-Au clusters and catalyzing the TMB-H_2O_2 chromogenic reaction are also important. However, this tendency would not be prolonged all the time. As shown in Fig. S11, the value A_0/A increased rapidly with the incubation time increasing up to 10 min, and then began to level off. So, 10 min was used as the optimal time for the incubation of Hg^{2+} and BSA-Au clusters. When the time for catalyzing the TMB-H_2O_2 chromogenic reaction changed from 0 to 10 min, the relative value of A_0/A increased greatly and then it reached a stable period. To obtain stable results, 15 min was chosen as the optimal time for catalyzing the TMB-H_2O_2 chromogenic reaction.

3.3. Analytical performance and detection of mercury content in cosmetic products

Under optimal experimental conditions, the calibration curve of the absorbance at 652 nm against the Hg^{2+} concentration was linear in a range from 10 nM (2 ppb) to 10 μM (2 ppm) with a detection limit of 3 nM (0.6 ppb, 3σ). The detection limit is much lower than the maximum level (1 ppm, ca. 4.98 μM) of mercury in cosmetics permitted by Ministry of Health of the People's Republic of China (GB/T 7917.1-1987) [18]. There was a linear relationship $A_0/A = 1.0561 + 0.5728C$, $R^2 = 0.9955$ (Fig. 4) between A_0/A and Hg^{2+} concentration. This calibration curve can be used for the quantitative determination of Hg^{2+} with high sensitivity. And the repeatability expressed as the relative standard deviation (RSD) was 1.5% ($n = 11$).

With an increasing Hg^{2+} concentration, visual fading of the blue color of TMB-H_2O_2 system appears (Fig. 5). As shown in Fig. 5, 4.98 μM (1 ppm), which is the maximum level of mercury in cosmetics permitted by the PR China, can be visually distinguished from other concentrations. Thus, our method is applicable to qualitative and semi-quantitative detection, and is available for rapid naked-eyed screening of large batches of cosmetics products without the aid of any instrumentation.

To examine the selectivity of the method, we investigate the interference from foreign species with the determination of 1.0 μM

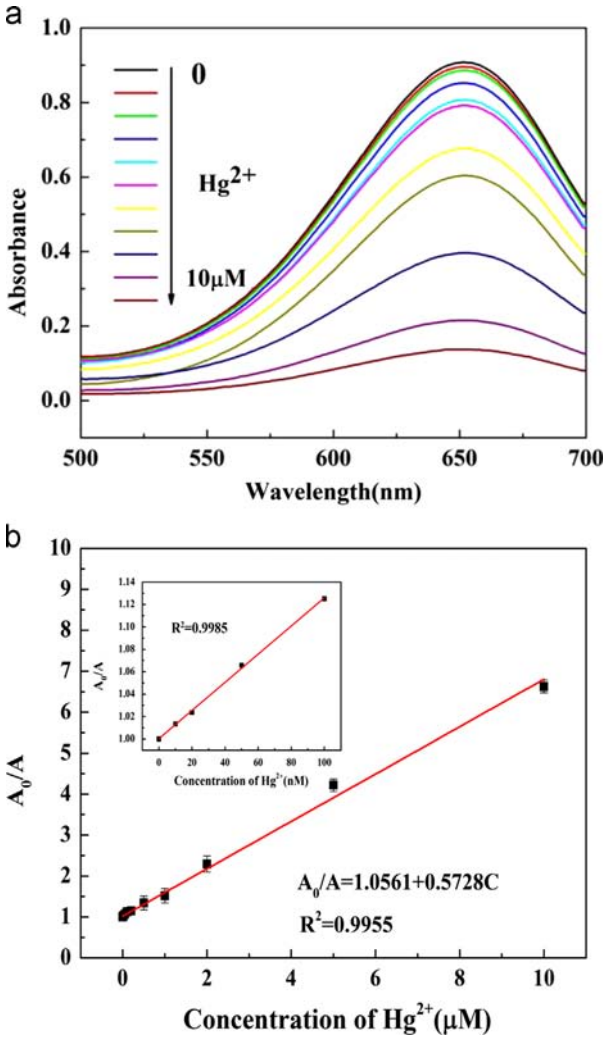

Fig.4. (a) Absorption spectra and (b) linear calibration plot for Hg^{2+} detection. Hg^{2+} concentrations were 0, 10 nM, 20 nM, 50 nM, 100 nM, 200 nM, 500 nM, 1 μM, 2 μM, 5 μM and 10 μM; Inset Hg^{2+} concentrations were 0, 10 nM, 20 nM, 50 nM, 100 nM; BSA-Au clusters, 200 μM; TMB, 150 μM; H_2O_2, 5 mM; temperature, 40 °C; pH 4.0. RSD = 1.5% (n = 11).

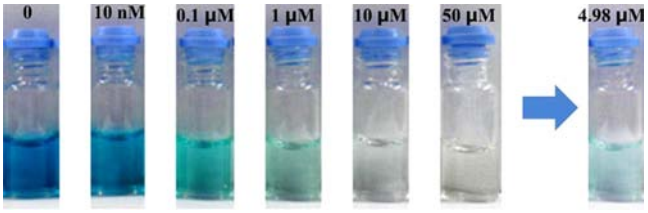

Fig. 5. Visual detection of Hg^{2+} 4.98 μM (1 ppm), which is the maximum level of mercury in cosmetics permitted by the PR China, can be visually distinguished from other concentrations.

Table 1
Determination of mercury in cosmetic products.

Samples	Results obtained by proposed method (ppm) ($n = 3$, $P = 0.90$)	Results obtained by AFS (ppm) ($n = 3$, $P = 0.90$)
1	124.1 ± 1.06	125.1 ± 1.72
2	0.044 ± 0.009	0.048 ± 0.004

Table 2
Comparison of our work with the previous colorimetric methods to detect Hg^{2+}.

Samples	Sensing materials	Methods	Linear range/limit of detection	References
Water	AuNPs stabilized with dithia-diaza ligands	UV–vis absorbance at 680 nm	0–9 μM/35 nM	Woravith et al. [29]
Water	AuNPs	UV–vis absorbance at 652 nm	1–600 nM/0.3 nM	Long et al. [9]
Water	Unmodified silver nanoparticles and mercury-specific oligonucleotides	UV–vis absorbance ($A_{570\ nm}/A_{395\ nm}$)	25–500 nM/17 nM	Wang et al. [30]
Water	Quaternary ammonium group-capped AuNPs	UV–vis absorbance ($A_{670\ nm}/A_{520\ nm}$)	0–600 nM/30 nM	Liu et al. [31]
Water	Mercaptopropionic acid-homocystine-AuNPs	UV–vis absorbance	2–100 ppb/2 ppb	Tan et al. [32]
Water	DNA and unmodified AuNPs	UV–vis absorbance ($A_{700\ nm}/A_{520\ nm}$)	0–5 μM/0.5 μM	Xu et al. [33]
Water	DNA-Functionalized AuNPs	Melting temperature	0–2 μM/100 nM	Lee et al. [34]
Water	DNA-functioned gold nanoparticles	Fluorescent analysis method	96–6400 nM/40 nM	Wang et al. [35]
Water	–	AFS	0–300 μg L^{-1}/0.2 μg L^{-1}	Zheng et al. [20]
Cosmetic	BSA-Au cluters	UV–vis absorbance at 652 nm	10 nM–10 μM/3 nM	Present method

(0.2 ppm) Hg^{2+}. The tolerable limit of an interfering species was taken as a relative error of less than ± 5%. It was found that Cd^{2+}, Al^{3+}, Cu^{2+}, Fe^{3+}, Cr^{3+}, Pb^{2+}, Ni^{2+}, Ag^{+}, Co^{2+}, Ca^{2+}, Mg^{2+}, K^{+}, and Zn^{2+} have no significant effect on the determination of Hg^{2+} even when they are present up to 50 to 1400 times the concentration ratio of Hg^{2+} (Table S1). Two commercial lightening creams were selected to be digested and the mercury levels in these products were detected by the proposed method and AFS, respectively. Sample 1 is an unqualified product that contains a higher mercury level than the maximum level in cosmetics permitted by the PR China. As shown in Table 1, results obtained by the two methods had no significant difference (P=0.90).

3.4. Comparison of our work with previous colorimetric methods to detect Hg^{2+}

Compared with previous reported detection methods, our approach is inexpensive and has reasonable sensitivity and selectivity (Table 2). Unlike most AuNP-based methods for sensing Hg^{2+} that involve a color change through the analyte-triggered aggregation of AuNPs, this method is based on the color change by the inhibition of catalytic activity of BSA-Au clusters. Therefore, the consumption of BSA-Au clusters is little. Most of the materials (e.g., TMB or H_2O_2) used in this assay are inexpensive and available commercially, making this assay particularly useful for resource-poor settings. The BSA-Au clusters are more stable than AuNPs in solutions with a high salt concentration (e.g., 1 M NaCl). The solvent could be removed by freeze-drying, and the BSA-Au clusters could be stored in the solid form [11]. Taking advantage of high sensitivity and significant color change at 4.98 μM (1 ppm) Hg^{2+} (Fig. 5), this method made it possible to estimate total mercury content in cosmetics by naked-eyed screening. TMB-H_2O_2 is a typical reaction that is often used in enzyme-linked immunosobent assay (ELISA). So the proposed assay can be potentially applied to develop the high-throughput screening by coupling with a microplate reader. Further work toward this direction is underway. Although the cosmetic product is chosen here to establish this assay by proof of principle experiments, our approach is readily transferable to other samples such as the quantitative determination of mercury in water.

4. Conclusions

In summary, we provide a colorimetric approach to detect Hg^{2+} with high sensitivity and selectivity. BSA-Au clusters possess peroxidase-like activity and can catalyze the chromogenic reaction of H_2O_2 and TMB. Furthermore, Hg^{2+} can interact with Au^{+} with high specificity, resulting in the inhibition of the enzymatic activity. The linear range of Hg^{2+} assay is from 10 nM (2 ppb) to 10 μM (2 ppm) and the detection limit is as low as 3 nM. Our presentation would help to develop a new application of BSA-Au clusters to Hg^{2+} detection by naked-eyed screening.

Acknowledgments

This research was supported by grants from the National Basic Research Program of China (Grant no. 2011CB933600), National Natural Science Foundation of China (No. 21175110), the Natural Science Foundation Project of CQ CSTC (Grant no. 2010BB4004).

Appendix A. Supplementary material

Supplementary data associated with this article can be found in the online version at http://dx.doi.org/10.1016/j.talanta.2013.08.053.

References

[1] L. Gao, J. Zhuang, L. Nie, J. Zhang, Y. Zhang, N. Gu, T. Wang, J. Feng, D. Yang, S. Perrett, X. Yan, Nat. Nanotechnol. 2 (2007) 577–583.
[2] Y.J. Song, K.G. Qu, C. Zhao, J.S. Ren, X.G. Qu, Adv. Mater. 22 (2010) 2206–2210.
[3] Y.J. Song, X.H. Wang, C. Zhao, K.G. Qu, J.S. Ren, X.G. Qu, Chem.-Eur. J. 16 (2010) 3617–3621.
[4] W. Shi, Q. Wang, Y. Long, Z. Cheng, S. Chen, H. Zheng, Y. Huang, Chem. Commun. 47 (2011) 6695–6697.
[5] W. He, X. Wu, J. Liu, X. Hu, K. Zhang, S. Hou, W. Zhou, S. Xie, Chem. Mater. 22 (2010) 2988–2994.
[6] Y. Jv, B. Li, R. Cao, Chem. Commun. 46 (2010) 8017–8019.
[7] Z. Dai, S. Liu, J. Bao, H. Ju, Chem.-Eur. J. 15 (2009) 4321–4326.
[8] H. Wei, E. Wang, Anal. Chem. 80 (2008) 2250–2254.
[9] Y.J. Long, Y.F. Li, Y. Liu, J.J. Zheng, J. Tang, C.Z. Huang, Chem. Commun. 47 (2011) 11939–11941.
[10] C.-W. Tseng, H.-Y. Chang, J.-Y. Changb, C.-C. Huang, Nanoscale 4 (2012) 6823–6830.
[11] J. Xie, Y. Zheng, J.Y. Ying, J. Am. Chem. Soc. 131 (2009) 888–889.
[12] C.V. Durgadas, C.P. Sharma, K. Sreenivasan, Analyst 136 (2011) 933–940.
[13] J. Xie, Y. Zheng, J.Y. Ying, Chem. Commun. 46 (2010) 961–963.
[14] X.X. Wang, Q. Wu, Z. Shan, Q.M. Huang, Biosens. Bioelectron. 26 (2011) 3614–3619.
[15] X.H. Zhang, J.G. Huang, Chem. Commun. 46 (2010) 6042–6044.
[16] Y.M. Olumide, A.O. Akinkugbe, D. Altraide, T. Mohammed, N. Ahamefule, S. Ayanlowo, C. Onyekonwu, N. Essen, Int. J. Dermatol. 47 (2008) 344–353.
[17] T.Y.K. Chan, Clin. Toxicol. 49 (2011) 886–891.
[18] Standard method of hygienic test for cosmetics mercury, Ministry of Health of the People's Republic of China. GB/T 7917.1-1987.
[19] R. Mathur, V. Balaram, S.S. Babu, Indian J. Chem., Sec. A: Inorg., Bio-inorg., Phys., Theor. Anal. Chem. 44 (2005) 1619–1624.

[20] C.B. Zheng, Y. Li, Y.H. He, Q. Ma, X.D. Hou, J. Anal. At. Spectrom. 20 (2005) 746–750.
[21] A. Burini, J.P. Fackler, R. Galassi, T.A. Grant, M.A. Omary, M.A. Rawashdeh-Omary, B.R. Pietroni, R.J. Staples, J. Am. Chem. Soc. 122 (2000) 11264–11265.
[22] V. Pershina, T. Bastug, T. Jacob, B. Fricke, S. Varga, Chem. Phys. Lett. 365 (2002) 176–183.
[23] Z. Huo, C.-K. Tsung, W. Huang, X. Zhang, P. Yang, Nano Lett. 8 (2008) 2041–2044.
[24] P. Pyykko, Angew. Chem. Int. Ed. 43 (2004) 4412–4456.
[25] M. Kim, T.J. Taylor, F.P. Gabbai, J. Am. Chem. Soc 130 (2008) 6332–6333.
[26] Z.Y. Zhang, A. Berg, H. Levanon, R.W. Fessenden, D. Meisel, J. Am. Chem. Soc. 125 (2003) 7959–7963.
[27] N. Wang, L.H. Zhu, D.L. Wang, M.Q. Wang, Z.F. Lin, H.Q. Tang, Ultrason. Sonochem. 17 (2010) 526–533.
[28] K. Murayama, M. Tomida, Biochemistry 43 (2004) 11526–11532.
[29] W. Chansuvarn, A. Imyim, Microchim. Acta 176 (2011) 57–64.
[30] Y. Wang, F. Yang, X. Yang, Mater. Int. 2 (2010) 339–342.
[31] D.B. Liu, W.S. Qu, W.W. Chen, W. Zhang, Z. Wang, X.Y. Jiang, Anal. Chem. 82 (2010) 9606–9610.
[32] Z.Q. Tan, J.F. Liu, R. Liu, Y.G. Yin, G.B. Jiang, Chem. Commun. (2009) 7030–7032.
[33] X. Xu, J. Wang, K. Jiao, X. Yang, Biosensors Bioelectron. 24 (2009) 3153–3158.
[34] J.S. Lee, M.S. Han, C.A. Mirkin, Angew. Chem. Int. 46 (2007) 4093–4096.
[35] H. Wang, Y.X. Wang, J.Y. Jin, R.H. Yang, Anal. Chem. 80 (2008) 9021–9028.